International Journal of Physics and Applications

E-ISSN: 2664-7583
P-ISSN: 2664-7575
IJOS 2024; 6(1): 89-96

www.physicsjournal.in
Received: 08-05-2024
Accepted: 11-06-2024

Halla Abbas Jasim
Department of Physics, College of Science, University of Thi-Qar, Thi-Qar, Iraq

Habeeb Allawi
Department of Physics, College of Science, University of Thi-Qar, Thi-Qar, Iraq

Corresponding Author:
Halla Abbas Jasim
Department of Physics, College of Science, University of Thi-Qar, Thi-Qar, Iraq

The effect of weak coronal mass ejections and their associated solar flares on the atmosphere

Halla Abbas Jasim and Habeeb Allawi

DOI: https://doi.org/10.33545/26647575.2024.v6.i2b.104

Abstract
This study selected 16 weak coronal mass ejections (CMEs) that were accompanied by X-class solar flares. likewise the six strongest solar flare events were chosen using data from the LASCO telescope on board the SOHO and GOES satellites, which indicated very high intensity during solar cycle 24. To study the effects of solar flare X-ray intensities on the ionosphere and thermosphere, an investigation is being conducted. The results demonstrate that the electron concentration reached its peak at an altitude of 260 km, measuring 7.14 e + 5 cm-3. Furthermore, the temperatures of electrons and ions during the flare were measured and determined to be 1897 k for electrons and 941 k for ions at an altitude of 260 km. These findings apply to all six events. Our findings indicate that feeble coronal mass ejections have minimal influence on the atmosphere, while powerful solar flares have a consistent or comparable impact across all occurrences.

Keywords: Coronal mass ejection**,** solar flare, atmosphere

1. Introduction
Large-scale explosions known as coronal mass ejections (CMEs) are extremely strong solar system phenomena that release a lot of magnetic field and energetic plasma into space. Many studies have demonstrated the correlations and noteworthy effects of CMEs on Earth, which are typically responsible for space weather [1-3]. Satellite malfunctions, broken power grids, and disruptions to communication and navigation systems are just a few of the high-tech human activities that are severely impacted by CMEs when they approach Earth and come into contact with the atmosphere. Furthermore, it has been demonstrated that variations in solar activity, such as solar flares and CMEs, have altered Earth's climate patterns by altering the amount of heat that the planet emits and receives [4, 5]. Large Angle and Spectrometric Coronagraph (LASCO) instrument on board Solar and Heliospheric Observatory (SOHO) spacecraft has been used for more than 25 years to observe and study CMEs in great detail [6]. Mostly seen through sunspots, solar flares represent a substantial component of solar activity. As active locations for space weather phenomena, such as solar flares and coronal mass ejections (CMEs), sunspots themselves do not generate radiation or particles that interact directly with Earth. Since magnetic reconnection causes massive quantities of energy to be released, solar flares are powerful explosions that happen in the solar corona and chromosphere. The abrupt rearrangement of magnetic field lines that occurs when two magnetic fields with opposing directions converge is known as magnetic reconnection, and it transforms stored magnetic energy into plasma kinetic or thermal energy. In 1946 [7, 8], Giovanelli made the initial proposal of this idea. On September 1, 1859, Carrington and Hodgman made the independent discovery of solar flares. Particle acceleration and coronal plasma heating (10–30 million Kelvin) are two phenomena linked to fluctuations in solar radiation that they saw. Earth's atmosphere is greatly impacted by solar flares, which release radiation throughout the electromagnetic spectrum, with a concentration in UV and X-ray emissions [9, 10]. Extreme UV radiation can increase by 4%–6% at the solar cycle's zenith, changing the composition of the stratosphere and altering air circulation patterns worldwide. Both the impulsive and progressive stages of solar flares are characterized by soft X-ray emissions that continue for a few minutes to many hours, and the impulsive phase, which emits hard X-rays, radio waves, and gamma rays while also accelerating electrons to energies beyond 1 MeV [11, 12]. Radiation from radio waves, microwaves, infrared, visible light, ultraviolet, X-rays, and gamma rays is used by astronomers to analyze distant occurrences.

The wavelength, frequency, and energy of these radiations are distinct [13, 14]. Based on intensity, solar flares are further classed within the X category, from X1 to X9, and from the strongest A and B classes to the most intense X class, as per the GOES classification [15].

Data and Methodology

443possible by the Sun's magnetic field. The Earth's magnetic field, known as the magnetosphere, functions as a barrier to keep solar events from reaching Earth. The Earth's molten outer core is the source of the electric currents that generate this field. Contrary to popular belief, the magnetic field is not a simple dipole but rather results from a self-sustaining dynamo process involving the spinning of conductive elements in the outer core.

The Earth's magnetic field varies, reaching a value of about 3.1x10-5 Tesla near the equator. The magnetosphere is pushed by solar winds to form the magnetopause, a boundary that is roughly ten times the radius of the Earth from its surface. Different currents, including the magnetopause, ring, and magnetotail currents, make up the magnetosphere. The magnetic field and space weather are greatly impacted by these currents [16-18].

Formation and Dynamics of the Ionosphere

As a result of solar radiation, particularly ultraviolet (UV) and X-ray radiation, gas atoms in the atmosphere ionize, forming the ionosphere. Ionization layers are produced as a result of the interaction between the solar radiation intensity and the density of gas atoms during the ionization process. Ionization and recombination processes balance each other out to define the electron density and general structure of the ionosphere. The rapid changes in ionization levels can result from solar flares or other cosmic occurrences that cause Sudden Ionospheric Disturbances (SIDs) [19]. Because of solar activity, the ionosphere exhibits diurnal oscillations, with higher levels of ionization during the day and lower levels at night. The information was acquired by means of the SOHO spacecraft's LASCO telescope for coronal mass ejections, the GOES satellites for solar flares, and the IRI for ionosphere data sets in [20-22].

Results and Discussions

In this study, a dataset was selected concerning weak coronal mass ejections (CMEs) during solar cycle 24, which were accompanied by strong solar flares at the same time, as shown in Table 1. We discovered 16 occurrences with X-class solar flares present, indicating extremely high intensity. All of the electromagnetic (EM) wave spectrum, from radio waves to gamma rays, is released by solar flares and coronal mass ejections (CMEs). Extreme energy outbursts have the potential to disrupt communications, power systems, GPS signals, and expose the upper atmosphere of the Earth to hazardous radiation.

Table 1: Solar flares of type X accompanied by weak coronal mass ejections.

No.	Solar Flare class	Date YYYY.MM.DD	Time UT	First seen of CME	Angular width Degree	Linear Speed Km/s
1	X2.14	2001\03\09	23:23	23:05	155	332
2	X3.03	2001\09\06	22:20	22:00	70	335
3	X1.45	2014\01\01	18:52	19:48	113	326
4	X1.45	2014\03\29	17:48	17:12	33	103
5	X1.99	2014\04\25	00:27	00:48	296	456
6	X1.43	2014\06\11	09:06	09:24	30	829
7	X1.58	2014\10\19	05:03	04:48	77	139
8	X1.39	2014\10\22	14:28	14:00	47	655
9	X4.58	2014\10\24	21:41	21:48	35	184
10	X1.5	2014\10\25	17:08	1736	49	171
11	X2.96	2014\10\27	14:47	15:12	55	170
12	X2.3	2014\11\07	17:26	17:12	87	469
13	X2.69	2014\12\20	00:28	01:25	36	286
14	X3.15	2015\03\11	22:11	20:57	13	294
15	X3.7	2017\09\06	09:10	09:48	80	391

Therefore, studying ionospheric responses to strong solar flares is an important topic in ionospheric physics and is thought to be a key component in improving positioning and navigation accuracy [15]. it is known that solar flares are the primary influence on the layers of the atmosphere. The electromagnetic radiation emitted simultaneously with the appearance of these flares has an effect on ionization and also increases the temperatures in some layers of the atmosphere, most notably the ionosphere. In this study, the six strongest solar flare events were also selected Table 2.

Event One

A solar flare with an intensity of (2.14*)* was observed on (2011/03/09) at (23:23) accompanied by a coronal mass ejection (CME) with a speed of (332 km/s) and an angular width of (155). By comparing the time and date with the IRI model and the specified region with coordinates over the city of Nasiriyah longitude (46) and latitude (31), it was observed from Figure 1 that there was an increase in electron concentration at the moment of the solar flare. The highest electron concentration was found to be (9.70 e + 4 cm-3) at an altitude of (300 km). Additionally, the temperatures of electrons and ions at the moment of the flare were recorded and found to be (1665 k) for electrons and (1051 k) for ions at an altitude of (300 km).

Table 2: The strongest events among the 16 events in Table 1.

No.	Solar Flare class	Date YYYY.MM.DD	Time UT	First seen of CME	Angular width Degree	Linear Speed Km/s
1	X2.14	2011\03\09	23:23	23:05	155	332
2	X3.03	2011\09\06	22:20	22:00	70	335
3	X4.58	2014\10\24	21:41	21:48	35	184
4	X2.3	2014\12\20	00:28	01:25	36	286
5	X3.15	2015\03\11	22:11	20:57	13	294
6	X3.7	2017\09\06	09:10	09:48	80	391

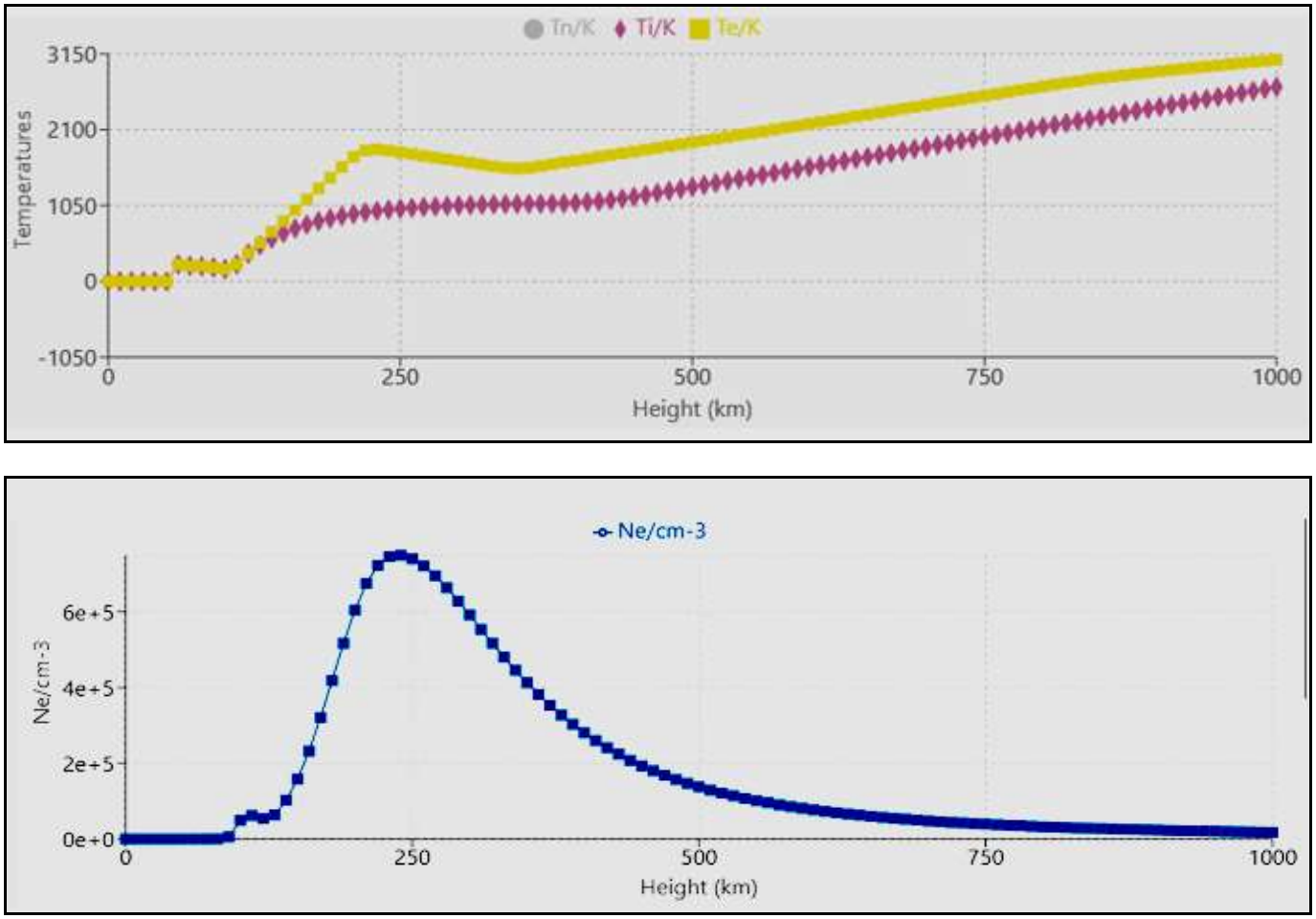

Fig 1a: Showing the electron concentration with altitude during a solar flare. 2011/03/09 at 23:23

Figure (1b): A figure showing the temperatures of both electrons and ions in the Earth's atmosphere during the solar flare on 2011/03/09 at 23:23

Event Two

A solar flare with an intensity of (3.03) was observed on (2011/09/06) at (22:20) accompanied by a coronal mass ejection (CME) with a speed of (335 km/s) and an angular width of (70). By comparing the time and date with the IRI model and the specified region with coordinates over the city of Nasiriyah longitude (46) and latitude (31), it was observed from Figure 1 that there was an increase in electron concentration at the moment of the solar flare. The highest electron concentration was found to be (2.92 e + 5 cm-3) at an altitude of (280 km). Additionally, the temperatures of electrons and ions at the moment of the flare were recorded and found to be (1530 k) for electrons and (8781 k) for ions at an altitude of (280 km).

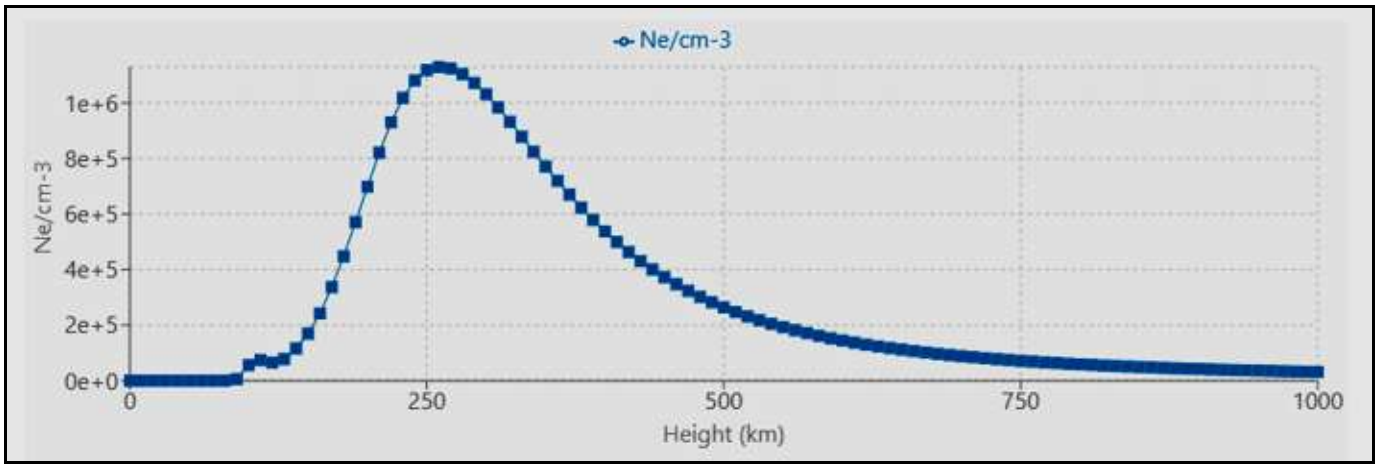

Fig 2a: Showing the electron concentration with altitude during a solar flare.in 2011\09\06 at 22:20

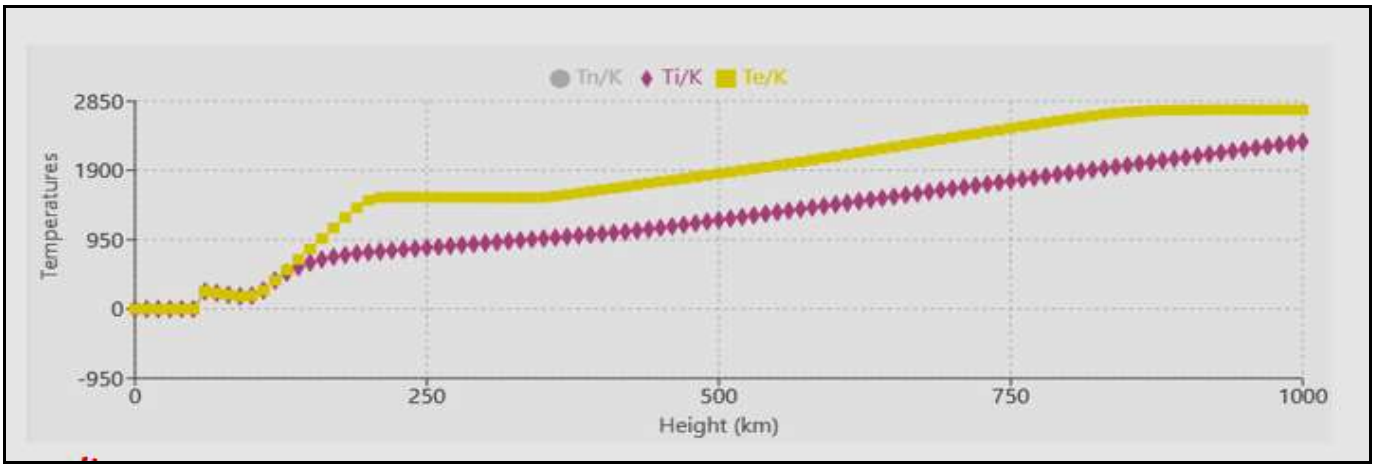

Fig 2b: A figure showing the temperatures of both electrons and ions in the Earth's atmosphere during the solar flare on 2011\09\06 at22:20

Event Three

A solar flare with an intensity of X4.58 was observed on (2014\10\24) at (21:41) accompanied by a coronal mass ejection (CME) with a speed of (184 km/s) and an angular width of (35). By comparing the time and date with the IRI model and the specified region with coordinates over the city of Nasiriyah longitude(46) and latitude(31), it was observed from Figure 1 that there was an increase in electron concentration at the moment of the solar flare. The highest electron concentration was found to be (1.29 e + 6 cm-3) at an altitude of (260 km). Additionally, the temperatures of electrons and ions at the moment of the flare were recorded and found to be (1648 k) for electrons and (1182 k) for ions at an altitude of (260 km).

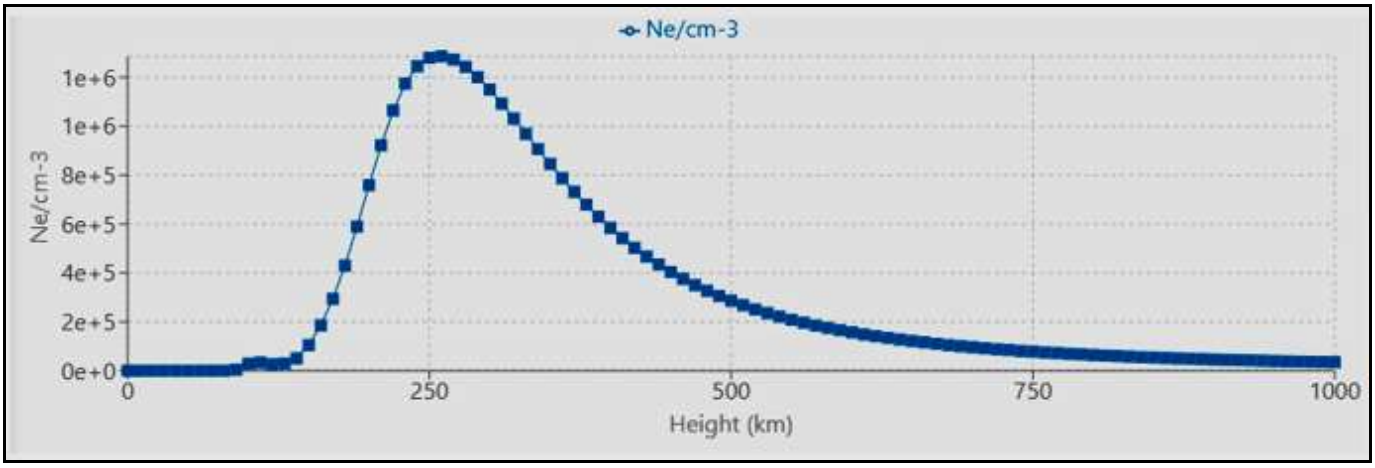

Fig 3a: Showing the electron concentration with altitude during a solar flare in 2014\10\24 at21:41

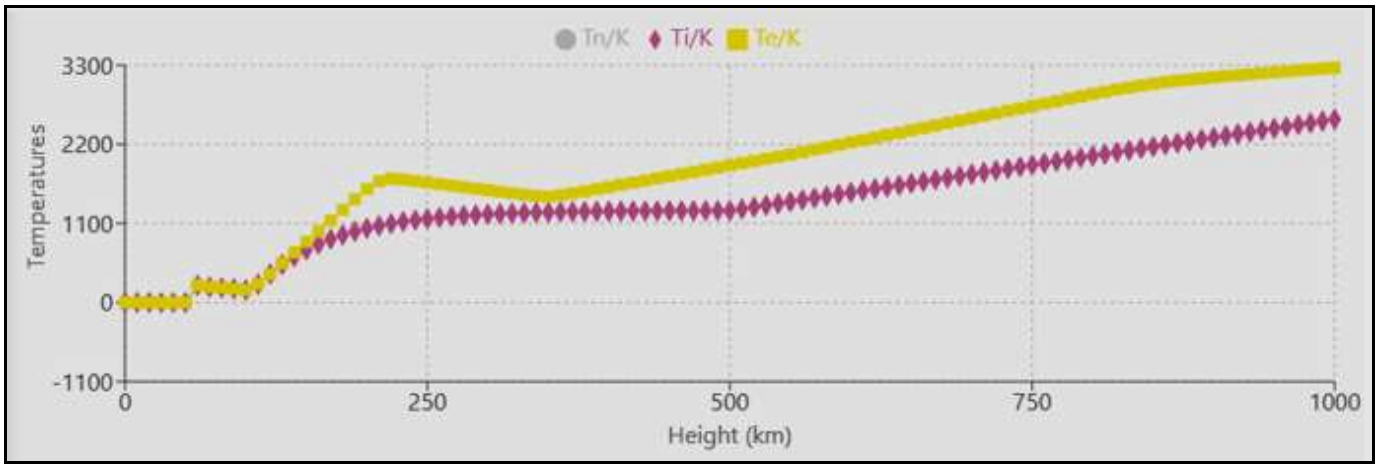

Fig 3b: A figure showing the temperatures of both electrons and ions in the Earth's atmosphere during the solar flare on 2014\10\24 at 21:41

Event Four

A solar flare with an intensity of (2.69) was observed on (2014\12\20) at (00:28) accompanied by a coronal mass ejection (CME) with a speed of (286 km/s) and an angular width of (36). By comparing the time and date with the IRI model and the specified region with coordinates over the city of Nasiriyah longitude (46) and latitude (31), it was observed from Figure 1 that there was an increase in electron concentration at the moment of the solar flare. The highest electron concentration was found to be (1.12 e + 6 cm-3) at an altitude of (250 km). Additionally, the temperatures of electrons and ions at the moment of the flare were recorded and found to be (1648 k) for electrons and (1173 k) for ions at an altitude of (250 km).

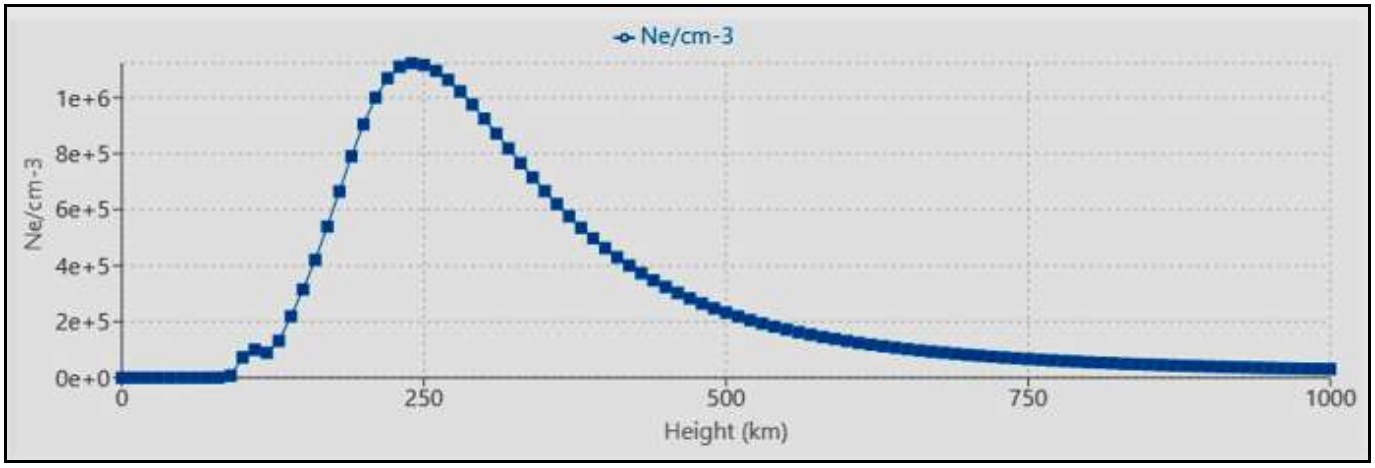

Fig 4a: Showing the electron concentration with altitude during a solar flare in 2014\12\20 at 00:28

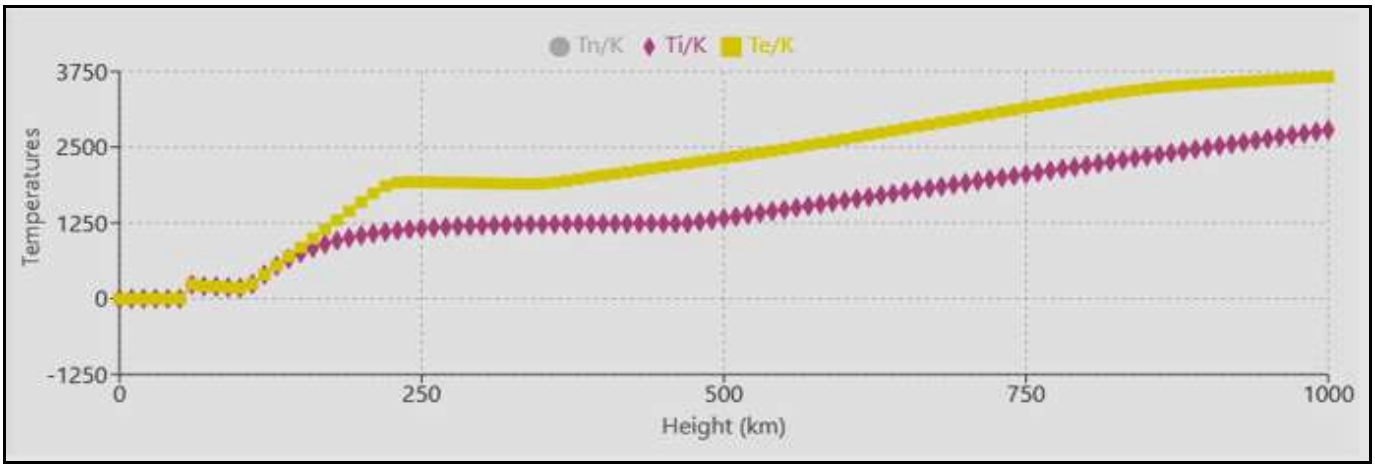

Fig 4b: A figure showing the temperatures of both electrons and ions in the Earth's atmosphere during the solar flare on in 2014\12\20 at 00:28

Event Five

A solar flare with an intensity of (3.15) was observed on (2015\03\11) at (22:11) accompanied by a coronal mass ejection (CME) with a speed of (294 km/s) and an angular width of (13). By comparing the time and date with the IRI model and the specified region with coordinates over the city of Nasiriyah longitude (46) and latitude(31), it was observed from Figure 1 that there was an increase in electron

concentration at the moment of the solar flare. The highest electron concentration was found to be (1.15 e + 6 cm-3) at an altitude of (310 km). Additionally, the temperatures of electrons and ions at the moment of the flare were recorded and found to be (942 k) for electrons and (913 k) for ions at an altitude of (310 km).

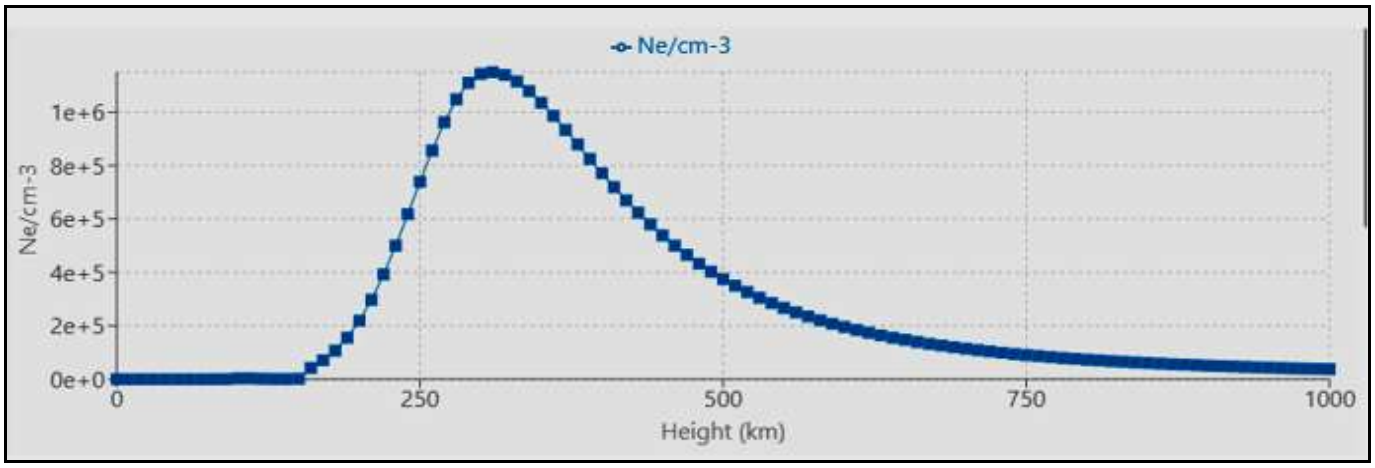

Fig 5a: Showing the electron concentration with altitude during a solar flare in 2015\03\11 at 22:11

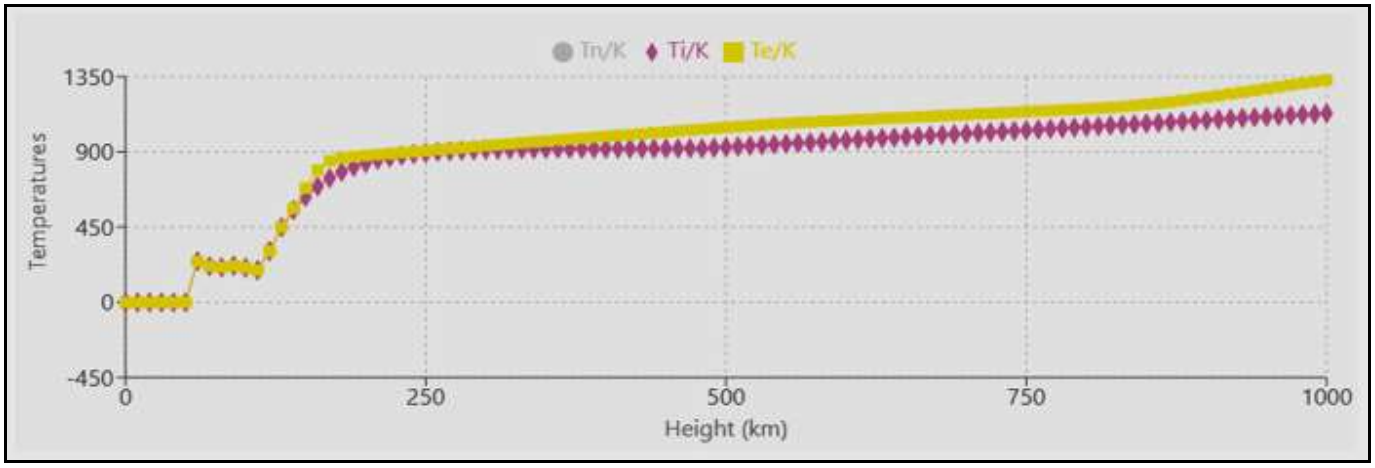

Fig 5b: A figure showing the temperatures of both electrons and ions in the Earth's atmosphere during the solar flare on 2015\03\11 at 22:11

Event Six

A solar flare with an intensity of (3.7) was observed on (2017\09\06) at (09:10) accompanied by a coronal mass ejection (CME) with a speed of (391 km/s) and an angular width of (80). By comparing the time and date with the IRI model and the specified region with coordinates over the city of Nasiriyah longitude(46) and latitude(31), it was observed from Figure 1 that there was an increase in electron concentration at the moment of the solar flare. The highest electron concentration was found to be (7.14 e + 5 cm-3) at an altitude of (260 km). Additionally, the temperatures of electrons and ions at the moment of the flare were recorded and found to be (1897 k) for electrons and (941 k) for ions at an altitude of (260 km).

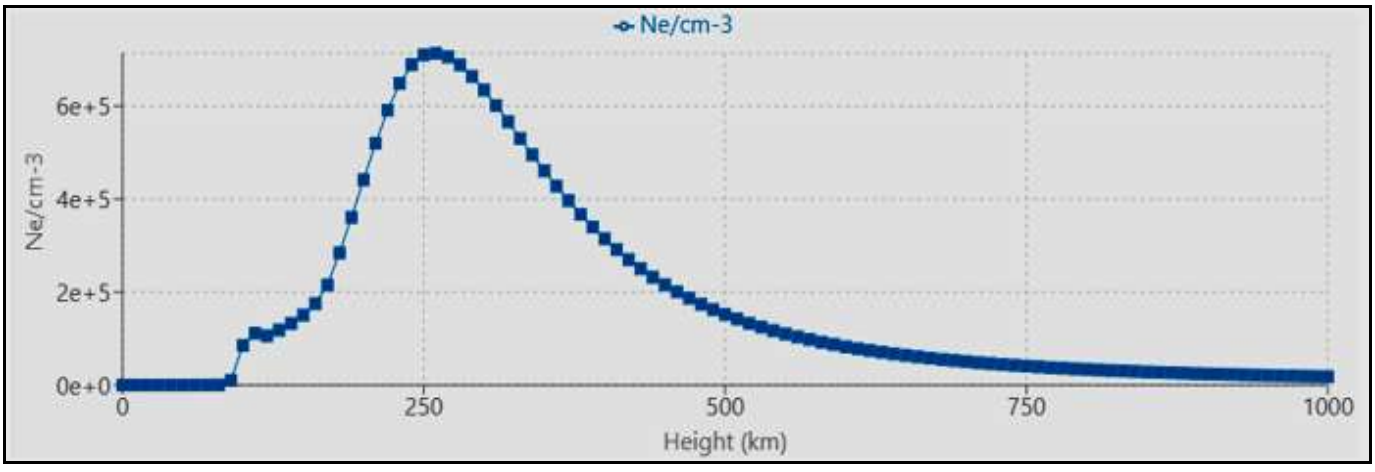

Fig 6a: Showing the electron concentration with altitude during a solar flare in 2017\09\06 at09:10

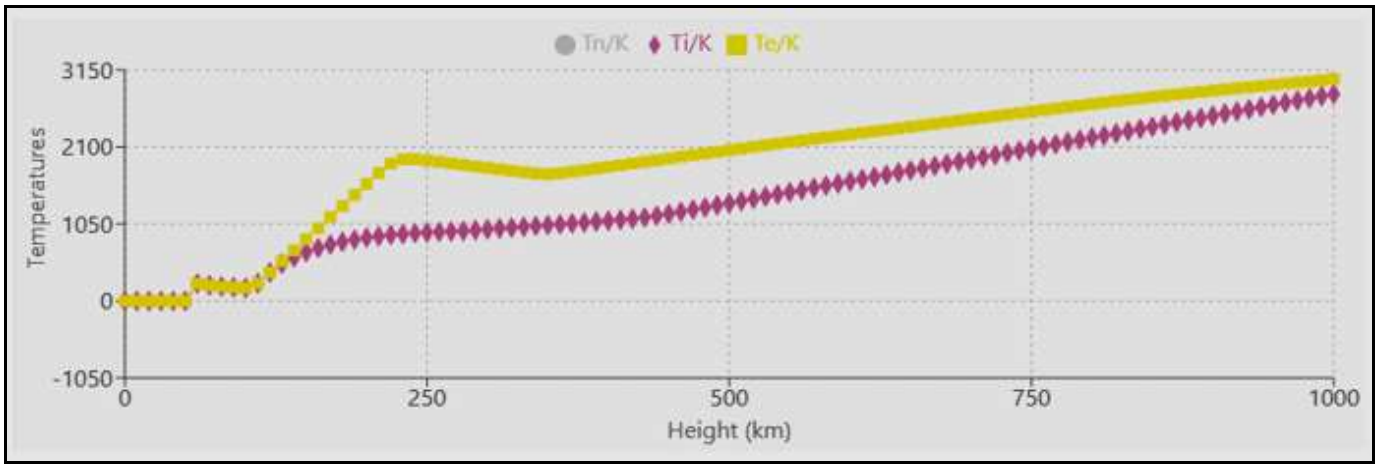

Fig 6b: A figure showing the temperatures of both electrons and ions in the Earth's atmosphere during the solar flare on same time

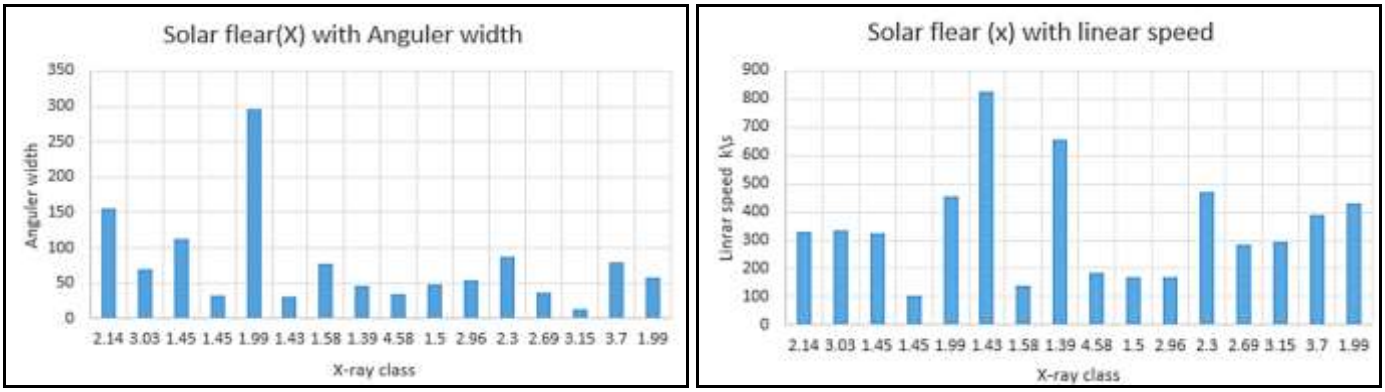

Fig 7: X rays solar flare intensity with coronal mass ejection linear speed (rightside) and with coronal mass ejection angular width (lift side)

Conclusions

Our results show that weak coronal mass ejections have barely any impact on the atmosphere, and that strong solar flares have the same or similar effect on all events. This is due to the fact that all of the events we've chosen fall into the X class, which is characterized by extremely high levels of electromagnetic radiation, which causes ionization in the atmosphere up to 260 km in latitude. Also as we could see from the Figure 7 shows that there is no correlation between the linear speeds and angular width of CMEs and the intensities of the solar flares that cause them

References

1. Bothmer V, Daglis IA, Pirjola R. Space weather effects on power grids. Space Weather Eff; c2007. p. 269-88.
2. Verma PL, Singh P, Singh P. Coronal mass ejections and disturbances in solar wind plasma parameters in relation with geomagnetic storms. J Phys Conf Ser. 2014;511(1):12060.
3. Gopalswamy N. Halo coronal mass ejections and geomagnetic storms. Earth Planets Space. 2009;61:595-7.
4. Ansor NM, Hamidi ZS. Effects of CME-induced geomagnetic storm on geomagnetic induced current at high and middle latitudes. J Phys Conf Ser. 2022;2287(1):12035.
5. Ansor NM, Hamidi ZS, Shariff NNM. The impact on climate change due to the effect of global electromagnetic waves of solar flare and coronal mass ejections (CMEs) phenomena. J Phys Conf Ser. 2019;1298(1):12019.
6. Brueckner GE. The Large Angle Spectroscopic Coronagraph (LASCO). Sol Phys. 1995;162:357.
7. Huang Y. The variations of geomagnetic energy and solar irradiance and their impacts on Earth's upper atmosphere; c2014.
8. Kumar P, Bhatt YC, Jain R, Shishodia YS. Solar flare and its interaction with the Earth atmosphere: An introduction. Phys Educ. 2015;31(2):6.
9. Isola C, Favata F, Micela G, Hudson HS. The correlation between soft and hard X-ray components in flares: from the Sun to the stars. Astron Astrophys. 2007;472(1):261-268.
10. Matsumoto H, Svensmark H, Enghoff MB. Effects of Forbush decreases on clouds determined from PATMOS-x. J Atmos Sol Terr Phys. 2022;230:105845. doi:10.1016/j.jastp.2022.105845.
11. Ruzmaikin A. Origin of sunspots. Space Sci Rev. 2001;95(1):43-53.
12. Lai A, Ng K. Machine learning for traffic management in urban transportation networks. arXiv:2211.15691. 2023.
13. Jabbari S. Origin of solar surface activity and sunspots. Stockholm University; c2014.
14. Petrosian V, Orlando E, Strong AW. Theoretical model of solar flares. ApJ. 2023;in press.
15. Hathaway DH. The solar cycle. Living Rev Sol Phys. 2015;12(1):4.
16. Finlay CC, *et al*. International geomagnetic reference field: the eleventh generation. Geophys J Int. 2010;183(3):1216-1230.
17. Cattell C, Glesener L, Leiran B, Dombeck J, Goetz K, Oliveros JCM, *et al*. Periodicities in an active region correlated with Type III radio bursts observed by Parker Solar Probe. Astron Astrophys; c2021. p. 650 doi:10.1051/0004-6361/202039510.
18. Battaglia AF, Hudson H, Warmuth A, Collier H, Jeffrey NLS, Caspi A, *et al*. The existence of hot X-ray onsets in

solar flares. Astron Astrophys. 2023;679 doi:10.1051/0004-6361/202039510.
19. Huang C. Ionosphere dynamics and applications. 2021.
20. Nogueira PAB, *et al*. Modeling the equatorial and low-latitude ionospheric response to an intense X-class solar flare. J Geophys Res Sp Phys. 2015;120(4):3021-3032.
21. Materassi M, Alberti T, Migoya-Orué Y, Radicella SM, Consolini G. Chaos and predictability in ionospheric time series. Entropy. 2023;25:368.
22. Genser A. Machine learning for traffic management in urban transportation networks. PhD Thesis, ETH Zurich, Zurich, Switzerland; c2022.